

Synthesis, crystal structure and magnetism of three novel copper(II) complexes with pyrazole-based ligands

Igor F. Santos, Guilherme P. Guedes¹, Luiza A. Mercante, Alice M.R. Bernardino, Maria G.F. Vaz^{*}

Universidade Federal Fluminense, Instituto de Química, 24020-141 Niterói, Rio de Janeiro, Brazil

ARTICLE INFO

Article history:

Received 4 November 2011
Received in revised form 22 December 2011
Accepted 23 December 2011
Available online 3 January 2012

Keywords:

Molecular magnetism
Pyrazole
Copper(II) complex
Crystal structure

ABSTRACT

In this work we present the synthesis, crystal structure and magnetic properties of three copper(II) pyrazole-based complexes. These compounds were prepared by reactions between the ligands (**L1** = 5-amino-1-phenyl-1*H*-pyrazole-4-carbonitrile, **L2** = 5-amino-1-(4-methoxyphenyl)-1*H*-pyrazole-4-carbonitrile and **L3** = Ethyl 5-amino-1-phenyl-1*H*-pyrazole-4-carboxylate) and CuCl₂·2H₂O using an appropriate solvent. The crystalline structures of [Cu(L1)₂Cl₂] (**1**), [Cu(L2)₂Cl₂] (**2**) and [Cu(L3)₂Cl₂] (**3**) showed that copper ion is coordinated by two pyrazolic ligands through pyridinic nitrogen atom and two chloride ions in a distorted square-planar geometry. The magnetic measurements revealed a paramagnetic behavior for (**1**) and weak antiferromagnetic coupling between copper(II) ions in (**2**) and (**3**). Due to the presence of labile chloride ions in the structures, these monomeric copper(II) complexes may be used as building blocks in the synthesis of molecular magnetic compounds.

© 2012 Elsevier B.V. All rights reserved.

1. Introduction

Pyrazoles and their derivatives are aromatic systems that have strong electron donor ability due to two chemically different nitrogen atoms (*N*-pyrrole and *N*-pyridine) [1]. Previously reports showed that this difference allows the interaction of the nitrogen atoms with specific proteins leading to distinct pharmacological activities. Due to this fact pyrazole and its derivatives are an important class of compounds that attracted widespread attention and are widely used in medicinal chemistry [2]. Besides, pyrazole is also a versatile ligand in coordination chemistry, since it exhibits twenty-two distinct coordination modes [3]. Complexes containing this kind of ligand are known since 1889 with the discovery by Büchner of an Ag(I) complex, [Ag(*pz*)]_{*n*}, where *pz* stands for pyrazole [4]. However, a new interest in these compounds arose in the 1980s with the publication of Trofimenko's work, which highlighted a rich coordination chemistry of pyrazole-based ligands [5].

Although several coordination modes of the transition metals to pyrazole, the synthesis of polynuclear compounds with pyrazole-substituted ligands is not trivial and the formation of mononuclear complexes is favored. Furthermore, monomeric complexes have attracted the interest of many research groups in order to develop

materials in which the peculiar properties of compounds can be tuned through modification in the organic ligand [6]. The investigation of these complexes has become an interesting research field due to their relevance in bioinorganic chemistry [7], catalysis [8] and luminescent materials [9]. In addition, monomeric compounds have also been studied in the molecular magnetism field because they can act as building blocks for supramolecular architectures [10]. In order to obtain molecular magnetic compounds there are several widespread strategies [11]. One of them consists on the synthesis of coordination compounds in which a labile ligand is coordinated to the metal, allowing its replacement by other ligand or preformed coordination compound [12]. This methodology is useful to connect discrete molecules turning them into a polynuclear structure. The magnetic interaction occurs between the spin carriers of each module through an organic binder. One of the interesting aspects of this methodology is the possibility to control connectivity and final architecture by choosing appropriate molecular bricks [13]. Therefore, the knowledge of crystal structure and magnetic properties of these building blocks is important for designing complex structures. Here we report the syntheses, crystal structures and magnetic properties of three novel copper(II) pyrazole-based complexes, which are potential candidates as building blocks for molecular magnetic compounds.

2. Experimental

2.1. Materials and methods

Analytical grade reagents were purchased from different sources and used without further purification. The melting points

^{*} Corresponding author. Address: Universidade Federal Fluminense, Instituto de Química, Outeiro de São João Batista, s/n, CEP 24020-150 Niterói, Rio de Janeiro, Brazil. Tel.: +55 21 2629 2354; fax: +55 21 2629 2129.

E-mail address: mariavaz@vm.uff.br (M.G.F. Vaz).

¹ Permanent address: Universidade Federal Rural do Rio de Janeiro, Instituto de Ciências Exatas, Departamento de Química, BR 465 – km 47, 23070-200 Seropédica, RJ, Brazil.

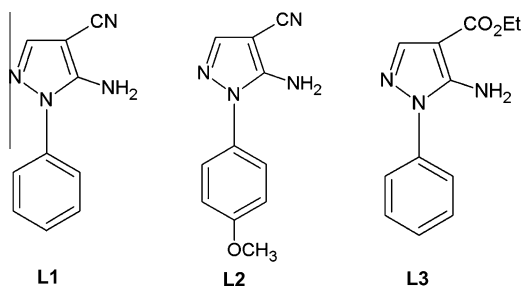


Fig. 1. Pyrazole-based ligands with *N*-donor substituents (nitriles and amines).

were determined in Fisatom digital device model 430. Elemental analyses were determined on a Perkin–Elmer 2400 CHN Elemental Analyzer. Nuclear magnetic resonance (NMR) spectrum was obtained at room temperature on a Varian Unity spectrometer operating at 500 MHz. The infrared spectrum was taken on a Spectrum One Perkin–Elmer spectrometer in the range of 4000–500 cm^{-1} , using KBr pellets. Magnetic measurements were performed on a Cryogenic SX-600 SQUID magnetometer in a range of 2–290 K with an applied field of 0.1 T. The sample was placed in a gelatin capsule and data were corrected for the diamagnetism and sample holder.

2.2. Syntheses

2.2.1. Preparation of the ligands L1–L3

The ligands **L1–L3** (Fig. 1) were synthesized following the procedures previously reported [14]. **L1** [15]: Yield: 90%. mp = 139–140 °C. IR (KBr, cm^{-1}): 3325 ($\nu_{\text{as}}(\text{NH}_2)$); 3225 ($\nu_{\text{s}}(\text{NH}_2)$); 2222 ($\nu_{\text{s}}(\text{CN})$); 1643–1535 (C=C/C=N). ^1H NMR (ppm): 7.63 (s, 1H); 7.41–7.57 (m, 5H); 4.5 (br, 2H). **L2**: Yield: 75%. mp = 144–145 °C. IR (KBr, cm^{-1}): 3359 ($\nu_{\text{as}}(\text{NH}_2)$); 3180 ($\nu_{\text{s}}(\text{NH}_2)$); 2214 ($\nu_{\text{s}}(\text{CN})$);

1658–1512 (C=C/C=N); 1257 (C–O). ^1H NMR (ppm): 7.60 (s, 1H); 7.38 (d, *J* 9.0 Hz, 2H); 7.00 (d, *J* 9.0 Hz, 2H); 3.8 (s, 3H). **L3** [16]: Yield: 80%. mp = 100 °C. IR (KBr, cm^{-1}): 3394 ($\nu_{\text{as}}(\text{NH}_2)$); 3263 ($\nu_{\text{s}}(\text{NH}_2)$); 1682 (C=O); 1627–1550 (C=C/C=N); 1280 ($\nu_{\text{as}}(\text{C–O})$); 1111 ($\nu_{\text{s}}(\text{C–O})$). ^1H NMR (ppm): 7.85 (s, 1H); 7.40–7.55 (m, 5H); 4.8 (br, 2H); 4.31 (q, *J* 7.2 Hz, 2H); 1.36 (t, *J* 7.2 Hz, 3H).

2.2.2. Preparation of the complexes

The reaction between $\text{CuCl}_2 \cdot 2\text{H}_2\text{O}$ with the ligands 5-amino-1-phenyl-1H-pyrazole-4-carbonitrile (**L1**), 5-amino-1-(4-methoxyphenyl)-1H-pyrazole-4-carbonitrile (**L2**) and ethyl 5-amino-1-phenyl-1H-pyrazole-4-carboxylate (**L3**) lead to the formation of monomeric copper complexes, namely $[\text{Cu}(\text{L1})_2\text{Cl}_2]$ (**1**), $[\text{Cu}(\text{L2})_2\text{Cl}_2]$ (**2**) and $[\text{Cu}(\text{L3})_2\text{Cl}_2]$ (**3**).

2.2.2.1. Preparation of compound (1). An ethanolic solution (20 mL) of $\text{CuCl}_2 \cdot 2\text{H}_2\text{O}$ (0.187 g, 1.1 mmol) was added slowly onto a solution containing 0.405 g (2.2 mmol) of **L1** in 10 mL of ethanol. The resulting solution was stored at 8 °C and red crystals were obtained after one week. Yield: 43%. mp = 167 °C. Anal. Calc. for $[\text{Cu}(\text{L1})_2\text{Cl}_2]$: C = 46.24%; H = 3.58%; N = 20.84%. Found C = 46.12%; H = 3.48%; N = 21.41%. IR (KBr, cm^{-1}): 3329 ($\nu_{\text{as}}(\text{NH}_2)$); 3234 ($\nu_{\text{s}}(\text{NH}_2)$); 2227 ($\nu_{\text{s}}(\text{CN})$).

2.2.2.2. Preparation of compound (2). A solution prepared by stirring 0.187 g (1.1 mmol) of $\text{CuCl}_2 \cdot 2\text{H}_2\text{O}$ in 20 mL acetonitrile was added slowly onto a solution containing 0.471 g (2.2 mmol) of **L2** in 10 mL of the same solvent. The resulting solution was stored at 8 °C and yellow crystals were obtained after four days. Yield 44%. mp = 215 °C. Anal. Calc. for $[\text{Cu}(\text{L2})_2\text{Cl}_2]$: C = 47.12%; H = 3.68%; N = 19.55%. Found C = 46.94%; H = 3.58%; N = 19.91%. IR (KBr, cm^{-1}): 3313 ($\nu_{\text{as}}(\text{NH}_2)$); 3240 ($\nu_{\text{s}}(\text{NH}_2)$); 2222 ($\nu_{\text{s}}(\text{CN})$); 1250 ($\nu_{\text{s}}(\text{OCH}_3)$).

Table 1

Summary of the crystal structure, data collection and refinement for compounds 1–3.

Identification	(1)	(2)	(3)
Formula	$\text{C}_{20}\text{H}_{18}\text{Cl}_2\text{CuN}_8\text{O}$	$\text{C}_{22}\text{H}_{20}\text{Cl}_2\text{CuN}_8\text{O}_2$	$\text{C}_{24}\text{H}_{26}\text{Cl}_2\text{CuN}_6\text{O}_4$
Molecular weight (g mol^{-1})	520.87	562.90	596.96
Temperature (K)	293	293	293
Wavelength (Å)	1.54180	0.71073	1.54180
Crystal system	Monoclinic	Triclinic	Monoclinic
Space group	$P2_1/n$	P-1	C2/c
<i>a</i> (Å)	7.5174(2)	7.4025(15)	7.92190(10)
<i>b</i> (Å)	16.7682(15)	8.7411(17)	17.7558(2)
<i>c</i> (Å)	17.7966(10)	10.546(2)	18.9725(3)
α (°)	90.0	66.60(3)	90.0
β (°)	95.133(3)	79.55(3)	97.0310(10)
γ (°)	90.0	67.67(3)	90.00
Volume (Å ³)	2234.3(2)	578.9(2)	2648.60(6)
<i>Z</i>	4	1	4
D_{calc} (g cm^{-3})	1.548	1.615	1.497
μ (mm^{-1})	3.84	1.21	3.38
<i>F</i> (000)	1060	287	1228
Crystal size (mm)	$0.26 \times 0.16 \times 0.07$	$0.04 \times 0.02 \times 0.01$	$0.30 \times 0.23 \times 0.11$
θ Range for data collection (°)	2.5–62.7	3.3–25.0	2.4–62.4
Reflections collected	6882	14993	17,344
Independent reflections/ R_{int}	3585/0.025	2044/0.074	2102/0.032
Data/restraints/parameters	3948/2/297	2044/2/168	2085/0/176
Goodness-of-fit on F^2	1.01	1.08	1.05
Final <i>R</i> indices [$I > 2\sigma(I)$]	$R1 = 0.038$ $wR2 = 0.106$	$R1 = 0.049$ $wR2 = 0.133$	$R1 = 0.030$ $wR2 = 0.082$
<i>R</i> indices (all data)	$R1 = 0.053$ $wR2 = 0.097$	$R1 = 0.067$ $wR2 = 0.1225$	$R1 = 0.0364$ $wR2 = 0.783$
Max peak/hole (e Å^{-3})	0.45/−0.34	0.48/−0.61	0.50/−0.43

For compound (1): $w = 1/[\sigma^2(\text{Fo}^2) + (0.0608\text{P})^2 + 1.725\text{P}]$; (2): $w = 1/[\sigma^2(\text{Fo}^2) + (0.055\text{P})^2 + 1.386\text{P}]$, (3): $1/[\sigma^2(\text{Fo}^2) + (0.0391\text{P})^2 + 4.2304\text{P}]$, where $\text{P} = (\text{Fo}^2 + 2\text{Fc}^2)/3$.

2.2.2.3. Preparation of compound (3). Compound (3) was synthesized under same conditions as (1), using the L3 ligand. Red single crystals were obtained after one week. Yield: 45%. mp = 184 °C. Anal. Calc. for [Cu(L3)₂Cl₂]: C = 48.29%; H = 4.39%; N = 14.08%. Found C = 48.14%; H = 4.36%; N = 13.95%. IR (KBr, cm⁻¹): 3441 (ν_{as}(NH₂)); 3333 (ν_s(NH₂)); 1705 (ν_s(C=O)); 1257 (ν_{as}(C–O)); 1111 (ν_s(C–O)).

2.3. X-ray crystallographic data

Single crystal X-ray diffraction data for compounds (1) and (3) were obtained on a Oxford GEMINI A Ultra with CCD diffractometer with Cu Kα radiation (λ = 1.54180 Å) at room temperature. Data collection, reduction and cell refinement were performed by CrysAlis RED program [17]. A multiscan absorption correction was applied [18]. The crystallographic data for (2) were collected on an Enraf Nonius Bruker KAPPA CCD diffractometer, using graphite monochromatic Mo Kα radiation (λ = 0.71069 Å). Final unit cell parameters were based on the fitting of all reflections positions using DIRAX [19]. Collected reflections were integrated using the EVALCCD program [20]. Empirical multiscan absorption corrections using equivalent reflections were performed with the SADABS program [21]. The structure solutions and full-matrix least-squares refinements based on F² were performed with the SHELXS-97 and SHELXL-97 program packages [22]. All atoms except hydrogen were refined anisotropically. Hydrogen atoms were treated by a mixture of independent and constrained refinement.

Table 2

Selected experimental bond distances (Å) and bond angles (°).

Compounds	Bond distance (Å)	Bond angle (°)	
(1)	Cu1–N5	1.979(3)	
	Cu1–N1	2.011(2)	
	Cu1–Cl1	2.2021(9)	
	Cu1–Cl2	2.2316(9)	
			N5–Cu1–N1
		N5–Cu1–Cl1	148.17(8)
		N1–Cu1–Cl1	92.62(7)
		N5–Cu1–Cl2	94.19(7)
		N1–Cu1–Cl2	141.79(8)
		Cl1–Cu1–Cl2	97.77(4)
(2)	Cu1–N2	1.967(3)	
	Cu1–N2i	1.968(3)	
	Cu–Cl1i	2.2557(14)	
	Cu–Cl1	2.2558(14)	
			N2–Cu1–N2 ⁱ
		N2–Cu1–Cl1 ⁱ	90.57(11)
		N2i–Cu1–Cl1 ⁱ	89.43(11)
		N2–Cu1–Cl1	89.43(11)
		N2 ⁱ –Cu1–Cl1	90.57(11)
		Cl1 ⁱ –Cu1–Cl1	180
(3)	Cu1–N2	2.0124(18)	
	Cu1–N2 ⁱⁱ	2.0124(18)	
	Cu1–Cl1	2.2358(6)	
	Cu1–Cl1 ⁱⁱ	2.2358(6)	
			N2–Cu1–N2 ⁱⁱ
		N2–Cu1–Cl1	157.17(6)
		N2 ⁱ –Cu1–Cl1	91.89(5)
		N2–Cu1–Cl1 ⁱⁱ	91.89(5)
		N2 ⁱ –Cu1–Cl1 ⁱⁱ	157.17(6)
		Cl1–Cu1–Cl1 ⁱⁱ	92.90(3)

Symmetry codes: (i) $-x, -y, -z$; (ii) $-x + 1, y, -z + 1/2$.

Table 3

Intermolecular interactions geometry.

Compounds	D–H...A	D–H	H...A	D...A	D–H...A
(1)	N3–H3B...O1w	0.86	2.32	2.985(4)	134
	N3–H3A...N8 ⁱ	0.86	2.23	3.081(4)	173
	O1w–H1w...Cl1 ⁱⁱ	0.81(2)	2.81(4)	3.456(3)	138(5)
	O1w–H2w...Cl2 ⁱⁱ	0.82(2)	2.51(3)	3.278(4)	156(6)
	N7–H7A...O1w ⁱⁱⁱ	0.86	2.37	2.962(4)	126
	N7–H7B...N4 ^{iv}	0.86	2.13	2.972(4)	168
	(2)	N3–H3...Cl1 ^v	0.861(10)	2.64(3)	3.380(5)
N3–H2...N4 ^{vi}		0.863(10)	2.239(17)	3.080(6)	165(5)
(3)		N3–H3B...Cl1 ^{vii}	0.87(3)	2.78(3)	3.509(2)
	N3–H3A...O1	0.80(3)	2.35(3)	2.936(3)	131(3)
	N3–H3A...Cl1 ^{viii}	0.80(3)	2.92(3)	3.475(2)	128(3)

Symmetry codes: (i) $x - 1/2, -y + 3/2, z + 1/2$; (ii) $-x - 1/2, y + 1/2, -z + 1/2$; (iii) $x + 1, y, z$; (iv) $x + 1/2, -y + 3/2, z - 1/2$; (v) $x + 1, y, z$; (vi) $-x + 1, -y + 1, -z - 1$; (vii) $x - 1/2, y - 1/2, z$; (viii) $-x + 1/2, y - 1/2, -z + 1/2$.

Details of data collection and structure refinement for compounds 1–3 are summarized in Table 1. Selected distances and angles are given in Tables 2 and 3.

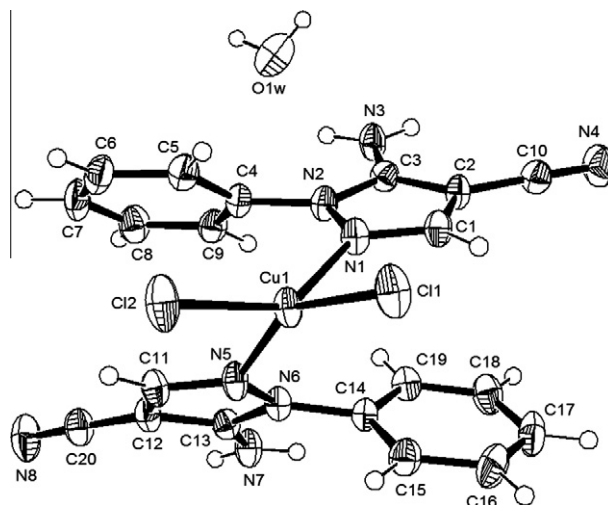


Fig. 2. ORTEP view of the molecular unit of compound 1. Ellipsoids are at 50% probability.

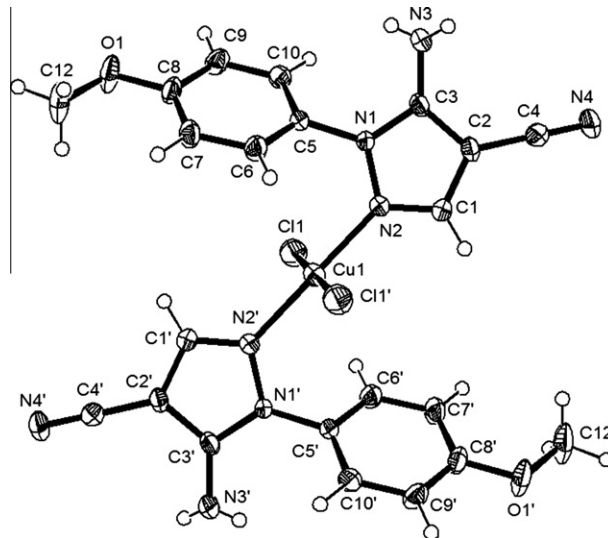


Fig. 3. ORTEP view of the molecular unit of compound 2. Ellipsoids are at 50% probability.

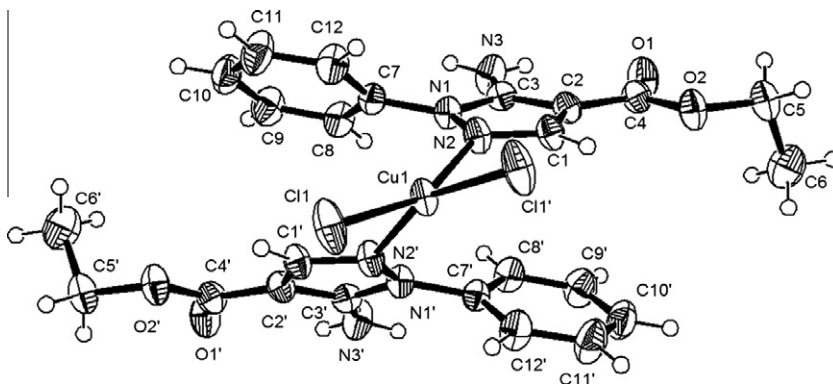


Fig. 4. ORTEP view of the molecular unit of compound **3**. Ellipsoids are at 50% probability.

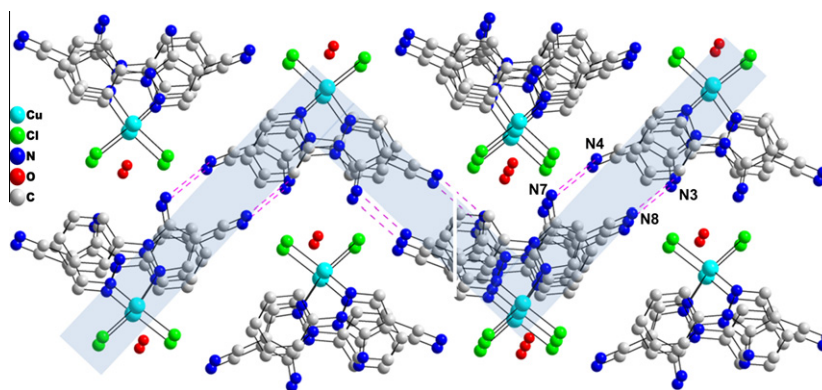


Fig. 5. Crystal packing of compound **1**. Hydrogen atoms were omitted for clarity.

3. Results and discussion

3.1. Structure descriptions

The molecular units of compounds **1–3** are shown in Figs. 2–4. In the three complexes, the copper(II) ion lies on a distorted square planar geometry, coordinated to two chloride ions and two ligand molecules through the pyridinic nitrogen atom of pyrazolic ring in a neutral monodentate mode [3]. In compounds (**1**) and (**3**) the copper(II) ion displays a *cis* geometry while in compound (**2**) the metal ion is in a *trans* geometry. The Cu–N and Cu–Cl bond lengths are typical when compared with those previously reported

[23]. The substituent groups in the 4 and 5 positions of the pyrazolic ring (amino and cyano for **L1** and **L2**, and amino and ester, for **L3**) have an important role in the crystal packing of the compounds **1–3** due to the establishment of a hydrogen bonded supramolecular network. Intermolecular short contacts parameters are given in Table 3. In the compound (**1**) the crystal packing is stabilized by intermolecular hydrogen bonds between the amino group and the lattice water molecule, with distance of 2.985(4) Å ($O1w \cdots N3$) and 2.962(4) Å ($O1w(x+1, y, z) \cdots N7$). In addition, intermolecular interactions between water hydrogen atoms and chloride ions with distances 3.456(3) Å ($O1w \cdots Cl1(x-1/2, y+1/2, -z+1/2)$) and 3.278(4) Å ($O1w \cdots Cl2(-x-1/2, y+1/2, -z+1/2)$) probably lead to a *cis* configuration on the complex. The crystal packing of (**1**) shows a supramolecular *zig-zag*

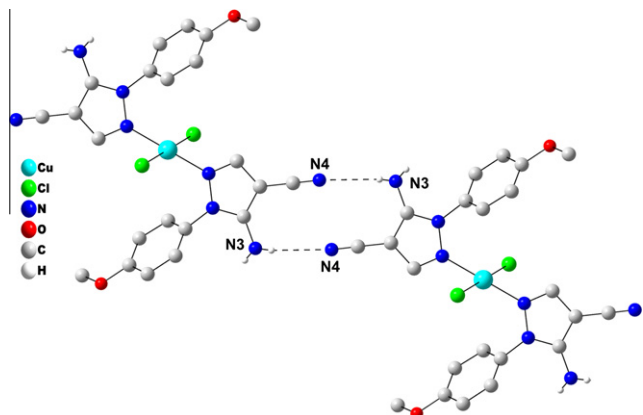


Fig. 6. Intermolecular hydrogen bonds in compound **2**. The hydrogen atoms except those involved in hydrogen bonding were omitted for clarity.

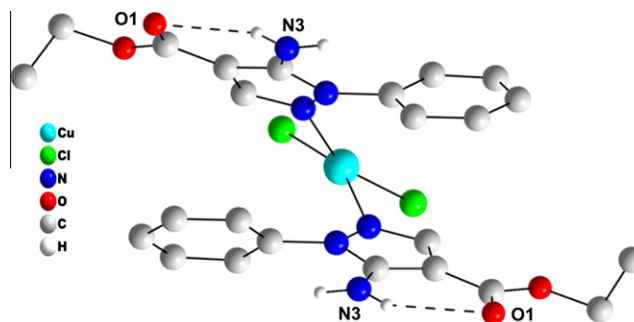


Fig. 7. Intramolecular hydrogen bond between the amino and carbonyl groups in compound **3**. The hydrogen atoms except those involved in hydrogen bonding were omitted for clarity.

chain-like structure as result of hydrogen bonds between amino and cyano groups (Fig. 5).

The X-ray structure of compound (2) shows that the copper(II) ion is coordinated to two L2 ligands, which has a methoxide substituent in the *para* position of the benzene ring. Intermolecular interaction between amine group and chloride ion with distance of 3.380(5) Å (N3...Cl1(x + 1, y, z)) is responsible to the *trans* configuration establishment in contrast to compounds (1) and (3).

Hydrogen bonds between amine and cyano groups are also present in this complex (Fig. 6). In the compound (3), the copper(II) ion displays a *cis* geometry as observed in (1). Weak interactions between chloride and amino group hydrogen atoms N3—H(3b)...Cl1(x - 1/2, y - 1/2, z) (2.78(3) Å) and N3—H(3a)...Cl1(-x + 1/2, y - 1/2, -z + 1/2) (2.92(3) Å) stabilize the crystal packing. Besides, intramolecular hydrogen bond interactions between amino and ester groups in 4 and 5 positions with distance of 2.350(5) Å (N3...O1) form a stable six members ring (Fig. 7). It is important to highlight that lattice water molecule and the substituent in the *para* position of the benzene ring play a key role in the crystal packing and probably are the main factors to lead to a *trans* geometry in compound (2), spite of the *cis* conformation of (1) and (3). In addition, the shortest intermolecular distances between copper ions are 8.401(7) Å (1), 7.4030(2) Å (2) and 7.922(4) Å (3).

3.2. Magnetic properties

The temperature dependences of the $\chi_M T$ products are displayed in Fig. 8. The experimental $\chi_M T$ values for compounds 1–3 at 290 K are 0.40 (1), 0.39 (2) and 0.41 cm³ K mol⁻¹ (3), close to the calculated one for $S = 1/2$ ion, with $g = 2.00$ (0.375 cm³ K mol⁻¹). These values remain constant from 290 to 8 K (1), 290 to 22 K (2) and 290 to 23 K (3) indicating a paramagnetic behavior in these temperature ranges. Upon cooling, $\chi_M T$ values decrease abruptly due to antiferromagnetic interactions. The reciprocal susceptibility versus temperature can be nicely fitted to the Curie–Weiss law ($\chi_M = C/(T - \theta)$) (insets Fig. 8). This analysis gives a Curie and Weiss constants of $C = 0.40$ emu mol⁻¹ and $\theta = -0.02$ K for (1), $C = 0.39$ emu mol⁻¹ and $\theta = -0.61$ K for (2), and $C = 0.40$ emu mol⁻¹ and $\theta = -0.42$ K for (3). The negative Weiss constants indicate the existence of a very weak antiferromagnetic coupling due to the intermolecular interactions, which connect the molecular units in the crystal lattice [24]. In order to taking into account the values of the magnetic coupling constant, the susceptibility magnetic data for (2) and (3) were reproduced considering a mean field approximation accordingly with the following expressions:

$$\chi_m = \frac{N\beta^2 g^2}{3kT} S(S + 1) \quad \chi_m^{MF} = \frac{\chi_m}{1 - zJ'\chi_m}$$

where zJ' is the intermolecular magnetic coupling constant. The best fit parameters were $g = 2.04$ and $zJ' = -1.70$ cm⁻¹ for compound (2) and $g = 2.08$ and $zJ' = -1.45$ cm⁻¹ for compound (3). Magneto-structural correlation for compounds 1–3 showed that the values of Weiss constant and the intermolecular magnetic coupling constant decrease as the distance between the copper ions increases, as expected. Compound (1) displays the longest distance between these ions, thus the lowest Weiss constant was obtained. Due to the paramagnetic behavior until 8 K, the magnetic data were not fitted as for (2) and (3). The comparison between compounds (2) and (3) shows the same tendency for the intermolecular magnetic coupling; in compound (2) the distance between copper ions is the shortest one, thus the intermolecular magnetic interactions are stronger when compared with compound (3).

4. Conclusion

In this work the syntheses, crystal structure and magnetic properties of three novel monomeric copper(II) pyrazole-based complexes were presented. Intermolecular and intramolecular interactions involving cyano, amine and ester groups play an important role for establishing a supramolecular network of hydrogen bonds in the compounds. We also showed that the change of the substituent in the *para* position of phenyl group bound to the 1-position of the pyrazole ring probably is the main

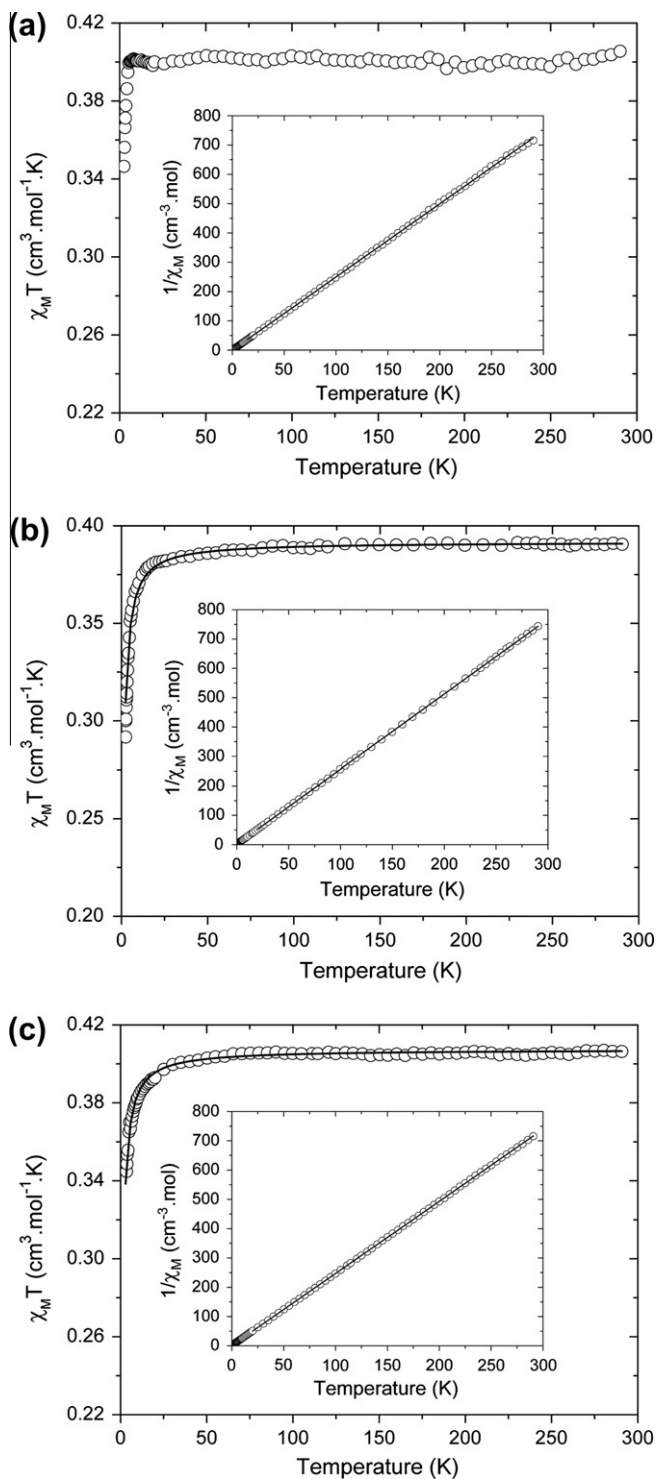


Fig. 8. Temperature dependences of $\chi_M T$ products of compounds 1 (a), 2 (b) and 3 (c). Solid lines in (b) and (c) represent the magnetic data fits. Insets: $1/\chi_M$ data as a function of the temperature fitted to the Curie–Weiss law (solid line).

reason that lead to the *trans* conformation of (2). Magnetic measurements revealed paramagnetic behavior for (1) and weak anti-ferromagnetic interactions for (2) and (3). This weak antiferromagnetic coupling can arise due the pathway provided by intermolecular interactions that connect the molecular units.

Supplementary material

CCDC ID: 851371 (1), 851372 (2), 851373 (3), contain the supplementary crystallographic data for this compound. These data can be obtained free of charge from the Cambridge Crystallographic Data Centre via www.ccdc.cam.ac.uk/data_request/cif.

Acknowledgements

Financial support from CAPES, FAPERJ, CNPq are kindly acknowledged. The authors also acknowledge the LDRX (Universidade Federal Fluminense), LabCri (Universidade Federal de Minas Gerais) for use of crystallographic facilities as well as Dr. Jackson A.L.C Resende for data collection of compound (2). We also thank Prof. Miguel A. Novak for the magnetic measurements.

References

- [1] L.C. Behr, R. Fusco, C.H. Jarboe, *The Chemistry of Heterocyclic Compounds – Pyrazoles, Pyrazolines, Pyrazolidines, Indazoles and Condensed Rings*, 1st ed., Interscience Publishers, New York, USA, 1967.
- [2] S.E. Sweeney, *Nat. Rev. Rheumatol.* 5 (2009) 475; G.L. Schieven, *Curr. Top. Med. Chem.* 5 (2005) 921; J. Saklatvala, *Curr. Opin. Pharm.* 4 (2004) 372; S. Kumar, J. Boehm, J.C. Lee, *Nat. Rev. Drug Disc.* 2 (2003) 717; D.M. Goldstein, Y.L. Kuglstatler, M.J. Soth, *J. Med. Chem.* 53 (2009) 2345; G. Wagner, S. Laufer, *Med. Res. Rev.* 26 (2006) 1; J. Westra, P.C. Limburg, *Mini-Rev. Med. Chem.* 6 (2006) 867.
- [3] A.M. Halcrow, *Dalton Trans.* (2009) 2059.
- [4] E. Büchner, *Ber. Dtsch. Chem. Ges.* 22 (1889) 842.
- [5] S. Trofimenko, *Chem. Rev.* 72 (1972) 497.
- [6] D.A. Souza, A.S. Florencio, J.W.M. Carneiro, S.S. Soriano, C.B. Pinheiro, M.A. Novak, M.G.F. Vaz, *Inorg. Chim. Acta* 361 (2008) 4024; T. Jurca, A. Farghal, P.-H. Lin, I. Korobkov, M. Murugesu, D.S. Richeson, *J. Am. Chem. Soc.* 133 (2011) 15814.
- [7] A. Golobiča, L. Ožbolta, F. Pohlevenb, I. Lebana, P. Šegedina, *Acta Chim. Slov.* 53 (2006) 238.
- [8] M.W. Jones, R.M. Adlington, J.E. Baldwin, D.D. Le Pevelen, N. Smiljanic, *Inorg. Chim. Acta* 363 (2010) 1097.
- [9] H.V.R. Dias, H.V.K. Diyabalanage, M.A. Rawashdeh-Omary, M.A. Franzman, M.A. Omary, *J. Am. Chem. Soc.* 125 (2003) 12072.
- [10] J. Pérez, L. Riera, *Eur. J. Inorg. Chem.* (2009) 4913; M.G.F. Vaz, L.M.M. Pinheiro, H.O. Stumpf, A.F.C. Alcântara, S. Golhen, L. Ouahab, O. Cador, C. Mathonière, O. Kahn, *Chem. Eur. J.* 5 (1999) 1486.
- [11] R.A. Allão, A.K. Jordão, J.A.L.C. Resende, A.C. Cunha, V.F. Ferreira, M.A. Novak, C. Sangregorio, L. Sorace, M.G.F. Vaz, *Dalton Trans.* 40 (2011) 10843; G. Marinescu, M. Andruh, F. Lloret, M. Julve, *Coord. Chem. Rev.* 255 (2011) 161; A. Dei, D. Gatteschi, C. Sangregorio, D. Shultz, L. Sorace, M.G.F. Vaz, *C. R. Chimie* 6 (2003) 663; G.A. Timco, T.B. Faust, F. Tuna, R.E.P. Winpenny, *Chem. Soc. Rev.* 40 (2011) 3067–3075.
- [12] G.P. Guedes, R.A. Allão, L.A. Mercante, M.G.F. Vaz, M.A. Novak, *Quim. Nova* 33 (2010) 1756.
- [13] J. Ferrando-Sori, D. Cangussu, M. Eslava, Y. Journaux, R. Lescouëzec, M. Julve, F. Lloret, J. Pasán, C. Ruiz-Pérez, E. Lhotel, C. Paulsen, E. Pardo, *Chem. Eur. J.* 17 (2011) 12482.
- [14] M.J. Dooley, R.J. Quirin, *Aust. J. Chem.* 42 (1989) 747; Y. Tominaga, J.K. Luo, L.W. Castle, R.N.J. Castle, *Heterocyclic Chem.* 30 (1993) 267.
- [15] J. Zukerman-Schpector, E.J. Barreiro, A.C.C. Freitas, *Acta Crystallogr., Sect. C: Cryst. Struct. Commun.* 50 (1994) 2095.
- [16] M. Zia-ur-Rehman, M.R.J. Elsegood, N. Akbar, R. Shah Zaib Saleem, *Acta Crystallogr., Sect. E: Struct. Rep. Online* 64 (2008) o1312.
- [17] RED CrysAlis, Oxford Diffraction Ltd., Version 1.171.32.38 (release 17.11.08 CrysAlis171.NET).
- [18] R.H. Blessing, *Acta Cryst. A* 51 (1995) 33.
- [19] A.J.M. Duisenberg, *J. Appl. Crystallogr.* 25 (1992) 92.
- [20] A.J.M. Duisenberg, L.M.J. Kroon-Batenburg, A.M.M. Schreurs, *J. Appl. Crystallogr.* 36 (2003) 220.
- [21] G.M. Sheldrick, SADABS, Program for Empirical Absorption Correction of Area Detector Data, University of Göttingen, Germany, 1996.
- [22] G.M. Sheldrick, T.R. Schneider, *Methods Enzymol.* 277 (1997) 319.
- [23] G.P. Guedes, F.F. Farias, M.A. Novak, F.L.A. Machado, M.G.F. Vaz, *Inorg. Chim. Acta* 378 (2011) 134; S. Mukherjee, C. Basu, S. Chowdhury, A.P. Chattopadhyay, A. Ghorai, U. Ghosh, H. Stoeckli-Evans, *Inorg. Chim. Acta* 363 (2010) 2752;.
- [24] P. Stachová, M. Korabik, M. Koman, M. Melník, J. Mrozinski, T. Glowiak, M. Mazúr, D. Valigura, *Inorg. Chim. Acta* 359 (2006) 1275.